의학박사 학위논문

Identification of key biologic pathways associated with glucocorticoid-induced bone mineral density changes in patients with asthma

천식 환자에서 스테로이드 사용에 따른 골밀도 변화 관련 주요 생물학적 경로 발굴

2020년 8월

서울대학교 대학원

의학과 협동과정 임상약리학과

이서영

ABSTRACT

Identification of key biologic pathways associated with glucocorticoid-induced bone mineral density changes in patients with asthma

Suh-Young Lee

Department of Clinical Pharmacology and Therapeutics

The Graduate School

Seoul National University

Derangement in bone mineral density (BMD) caused by glucocorticoids is well known. The present study aimed to identify key biological pathways associated with low BMD after glucocorticoid treatment in asthmatics using gene expression profiles of peripheral blood cells. We used immortalized B cells (IBCs) from 32 childhood asthmatics after multiple oral glucocorticoid bursts and peripheral blood mononuclear cells (PBMCs) from 17 adult asthmatics after long-term use of oral glucocorticoids. We searched for co-expressed gene modules

significantly related with the BMD Z score in childhood asthmatics and tested if these gene modules were preserved and significantly associated with the BMD Z score in adult asthmatics too. We identified a gene module composed of 199 genes significantly associated with low BMD in both, childhood and adult asthmatics. The structure of this module was preserved across gene expression profiles. We found that the cellular metabolic pathway was significantly enriched in this module. Among the 18 hub genes in this module, we postulated that 2 genes, *CREBBP* and *EP300*, contributed to low BMD following a literature review. A novel biologic pathway identified in this study highlighted a gene module and several genes that play possible roles in the pathogenesis of glucocorticoid-induced derangement in BMD.

Key words: Asthma, Bone, Density, Gene expression, Glucocorticoid

Student Number: 2013-31173

Contents

Abstract (English) ····· i

Introduction ····· 1

Methods ····· 5

Results ····· 17

Discussion ····· 21

References ····· 63

Abstract (Korean) ····· v

List of tables

Table 1. ····· 29

Table 2. ····· 31

Table 3. ····· 32

Table 4. ····· 34

Table 5. ····· 37

Table 6. ····· 41

Table 7. ····· 42

Table 8. ····· 45

Table 9. ····· 46

List of Figures

Figure 1. ····· 51

Figure 2. ····· 52

Figure 3. ····· 53

Figure 4. ····· 54

Figure 5. ····· 55

Figure 6. ····· 57

Figure 7. ····· 58

Figure 8. ····· 69

Figure 9. ····· 60

Figure 10. ····· 62

Introduction

Derangement in bone mineral density (BMD) caused by glucocorticoids is well known. Glucocorticoid treatment is the most common cause of secondary osteoporosis (1) and can induce dosage-dependent reduction in bone mineral accretion in childhood asthmatics (2). In general, the mechanisms of glucocorticoid action in bones are characterized by increased bone resorption and inhibition of bone formation (3). BMD is highly heritable, with heritability estimates of 0.5-0.9 (4). Glucocorticoids stimulate osteoclastogenesis by increasing the expression of RANK ligand and decreasing the expression of its decoy receptor, osteoprotegerin, resulting in increased bone resorption. Glucocorticoids also decrease osteoblastic function through the modulation of growth factor expression, receptor binding, or binding protein levels, thereby affecting bone formation (3).

Despite these common mechanisms, there exist individual differences in glucocorticoid sensitivity on bone physiology. Gene expression studies have been successfully applied to elucidate various biological processes with respect to responses to glucocorticoids and the deterioration of bone tissues. Polymorphisms in the gene encoding the glucocorticoid receptor modulate glucocorticoid sensitivity associated with certain phenotypes such as those with increased risk of cardiovascular diseases, increased body mass index, and major depression (5). Differences in glucocorticoid sensitivity can influence the

outcome and adverse effects of glucocorticoid therapy (6). It has also been reported that the effect of glucocorticoids on bones presents in varying degrees among individuals due to genetic factors which have the potential to modify the effects of oral corticosteroids (OCSs) on bone (7). We previously reported that polymorphisms in *CRHR1*, *TBCD* and *RAPGEF5* were associated with low BMD in childhood asthmatics after long-term treatment with glucocorticoids (7-9). In these studies, a gene-by-oral corticosteroid (OCS) interaction genome-wide association study (GWAS) was performed to identify genetic factors influencing OCS dose effects on bone mineral accretion in children with asthma. Top ranked single nucleotide polymorphisms (SNPs) in the GWAS were selected and whether these SNPs had regulatory effects on dexamethasone-induced gene expression in human primary bone cells was determined via an association test using a linear regression model (7, 9). However, to date, there has been no comprehensive study to elucidate the biologic mechanisms underlying glucocorticoid-induced derangement in BMD in asthmatics that are frequently treated with glucocorticoids.

Network-based analysis is an emerging approach that provides a straightforward representation of interactions between genes (10, 11), proteins (12), and cells (13). In gene co-expression networks, each gene corresponds to a node and each co-expression network corresponds to an adjacency matrix (14). The adjacency matrix encodes the connection strength between nodes. Nodes are connected if the corresponding genes are significantly co-expressed across

tissue samples. In an un-weighted analysis, gene co-expression is encoded using binary information (connected=1, unconnected=0). This 'hard' threshold causes loss of information and sensitivity. In weighted gene co-expression network analysis (WGCNA), a general framework for 'soft' thresholding that weighs each connection by a number in [0,1] is used. There is evidence that weighted networks can yield more robust results than unweighted networks (14). In these networks, highly connected nodes can represent essential genes that may contribute to a disease or phenotype. Through the integration of gene expression data and genotype data with advanced technology, we can identify functional genetic variants underlying disease pathogenesis. WGCNA transforms gene expression data into networks - known as modules - containing groups of genes with similar biological functions. It provides information comparing differentially expressed genes and interactions between genes in different co-expression modules and is useful for identifying potential biomarkers and therapeutic targets for numerous biological processes in various diseases such as cancers (15), schizophrenia (16), intracranial aneurysm (17), chronic kidney diseases (18), and allergic asthma (19).

With regard to bone metabolism and osteoporosis, many biological pathways affecting BMD have been identified via gene functional analysis using proteomics and genomic approaches (20-22). Wnt signaling pathway, Hedgehog signaling pathway, and mitogen-activated protein kinase and the calcium signaling pathways have been identified as significantly enriched

pathways involved in osteoporosis. A network based analysis also provided new insights into BMD genetics by grouping genes into modules that are enriched for particular biological processes (23, 24). However, to date, co-expression analysis for glucocorticoid-induced derangement in BMD is still insufficient to explain its underlying mechanisms.

The purpose of this study was to construct a gene co-expression network to predict clusters of candidate genes involved in the pathogenesis of derangement in BMD induced by glucocorticoids and to identify key biological pathways associated with low BMD after glucocorticoid treatment in patients with asthma. To achieve this goal, we used WGCNA with gene expression profiles of immortalized B cells (IBCs) from childhood asthmatics along with gene expression profiles of peripheral blood mononuclear cells (PBMCs) from adult asthmatics.

Methods

All experimental protocols were approved by the institutional review boards of the corresponding institutions. This study was approved by the Institutional Review Board of the Brigham and Women's Hospital (2002-P-00331/41) and the Seoul National University Hospital (H-1508-095-695). Informed consent was obtained from all study participants and a parents and/or legal guardians, if subjects were under 18 years of age. All procedures were carried out in accordance with relevant guidelines and regulations. The overall study design is presented in Figure 1.

1-1. Discovery data set

The discovery cohort consisted of non-Hispanic white children – whose IBCs were available - from the Childhood Asthma Management Program (CAMP) trial (25). Between December 1993 and September 1995, 1041 children aged 5 – 12 years were enrolled at eight clinical centers. The children had mild-to-moderate asthma, as defined by the presence of symptoms or by the use of an inhaled bronchodilator at least twice in a week or the use of daily medication for asthma. Their airway responsiveness to methacholine, as indicated by the concentration of the drug that caused a 20 percent decrease in the FEV_1, was 12.5 mg/mL or less. They had no other clinically significant conditions. The children's parents or guardians signed an informed consent form approved by

the local institutional review board. Follow-up visits occurred two and four months after randomization and at four-month intervals thereafter. In asthma exacerbations, short courses of oral prednisone were prescribed as per protocol. Each burst consisted of 2 mg/kg per day (up to 60 mg) of prednisone for 2 days followed by 1 mg/kg per day (up to 30 mg) for 2 days. Subsequent administration of prednisone was allowed when the improvement was insufficient.

1-2. Replication data set

The replication cohort was drawn from adult asthmatic patients who were treated at the Seoul National University Hospital, Seoul, Korea. Through a retrospective chart review, we identified subjects with asthma who had received more than 15 mg of prednisolone per day continuously for at least one year before enrollment, in order to ameliorate their symptoms. This dose was selected on the basis of a research claiming that doses above 10 mg of prednisolone per day resulted in significant bone loss (26). Patients with thyroid diseases, rheumatoid arthritis, diabetes, hepatic or renal dysfunctions, Cushing's syndrome, malignancies, cardiovascular diseases, Crohn's disease, ulcerative colitis, and history of surgery that may affect the absorption of drugs were excluded. Individuals with a history of hypersensitivity to OCS and vulnerable subjects were also excluded. The patients signed an informed

consent form approved by the local institutional review board. We estimated the number of target subjects based on previous case-control studies identifying significant biological pathways using a system biological method with gene expression array data of less than 30 patients (27, 28). Since the present study has an exploratory rationale, we intended to conduct our research with the minimum number of subjects within the scope to meet our purpose.

We collected peripheral blood samples from the patients when their disease condition was stable. Approximately 30 mL of blood was obtained from each patient using BD Vacutainer tubes containing acid-citrate-dextrose anticoagulant solution A (ACD-A; BD). The blood level of vitamin D in their blood was measured.

2. BMD measurement

BMD measurements of the lumbar spine (L1-L4) were performed annually during the study period by means of dual-energy x-ray absorptiometry [Hologic (Hologic Inc., Waltham, MA, US) or Lunar (GE Healthcare, Madison, WI, US)] in the childhood asthma cohort. The BMD Z score, which represents the difference between the measured bone density in a subject and the average bone density in age- and sex-matched controls, was calculated using the CAMP internal references (2). The final BMD Z score measured after a mean follow-up duration of 4.3 years was used as a target phenotype.

In the adult asthma cohort, BMD was measured at the lumbar spine (L1-L4) using dual-energy X-ray absorptiometry [Lunar (GE healthcare, Madison, WI, US)] upon the enrollment. Similar to childhood asthmatics, the BMD Z score was used as a target phenotype.

3. Isolation of PBMC and RNA

As previously described (29) IBCs derived from childhood asthmatics from the CAMP trial were cultured in RPMI 1640 medium. For adult asthmatics cohort, PBMCs were isolated from peripheral blood using Ficoll-Paque. ACD-A anticoagulated blood was centrifuged at 1800 rpm for 10 min and the top layer containing plasma was removed. The remaining blood was diluted with an equal volume of phosphate-buffered saline, pH 7.4 (PBS), containing 0.05 M ethylenediaminetetraacetic acid (EDTA; Invitrogen). 12.5 mL of diluted blood was layered over 25 mL of the Ficoll-Paque PLUS (GE Healthcare). Gradients were centrifuged at 1500 rpm for 30 min at room temperature in a swinging-bucker rotor without the brake applied. The PBMC interface was carefully removed by pipetting and washed with PBS-EDTA by centrifugation at 1800 rpm for 10 min. PBMC pellets were suspended in ammonium-chloride-potassium (ACK) lysing buffer (Invitrogen) and incubated for 10 min at room temperature with gentle mixing to lyse contaminating red blood cells. This was followed by a wash with PBS-EDTA. PBMC were cryopreserved in liquid

nitrogen in fetal calf serum (FCS; Invitrogen) containing 10 % dimethyl sulfoxide (DMSO; Thermo Fisher Scientific) and stored. PBMCs from adult asthmatics were cultured in RPMI 1640 medium for 6 hours (Sham-treated PBMCs). RNA was simultaneously extracted from PBMC and purified using the AllPrep RNA Mini Kit (Qiagen, Hilden, Germany) following the manufacturer's instruction. RNA quantitation and quality were determined using an Agilent 2100 Bioanlyzer according to the manufacturer's manuals.

4. Gene expression array

Gene expression levels were measured using the Illumina HumanRef8 v2 BeadChip (Illumina, San Diego, CA, US) for childhood asthmatics and the Affymetrix GeneChip Human Gene 2.0 ST (Affymetrix, Santa Clara, CA, US) for adult asthmatics. Affymetrix GeneChip Human Gene 2.0 ST contains over 1.35 million probe sets representing all exons of ~33,500coding transcripts of annotated genes and ~11,000 long intergenicnon-coding transcripts. Hybridization with the biotin-labeled RNA, staining and scanning of the chips followed the prescribed procedure outlined in the Affymetrix technical manual available at http://media.affymetrix.com/support/downloads/manuals/wt_expressionkit_manual.pdf;http://media.affymetrix.com/support/downloads/manuals/wt_term_label_ambion_user_manual.pdf. Hybridization was performed at 45 ℃ for 16

h using the Hybridization Oven 640 (Affymetrix). Washing and staining were done on a Fluidics Station 450 and images were acquired using the Affymetrix 7G GeneChip scanner. Procedures were performed according to the MIAME (Minimum Information About a MicroarrayExperiment) guidelines. We removed probes with bad chromosome annotation and probes in X or Y chromosome. We then did variance stabilizing transformation and quantile normalization respectively to reduce the effects of technical noises and to make the distribution of expression level for each array closer to normal distribution.

5. Identification of co-expression gene modules

Analysis was performed using R version 3.4.3 (www.r-project.org). We performed WGCNA on each gene expression profile using the R package “WGCNA” (30) to identify cluster modules of highly correlated genes.

To allow comparability of data from different microarray platforms, we first calculated the mean expression value of each gene in the two expression profiles (IBCs and PBMCs) after collapsing probes by genes. We then compared the mean expression levels of those genes and selected the top-5000 genes in common with the highest correlation. Using 5,000 genes, we first characterized unsigned correlation networks and their relationships with each other and found gene modules in the gene expression profiles from childhood asthmatics. The soft-thresholding power b was calculated during the

construction of each module using the pickSoftThreshold function of the WGCNA. This method provided a suitable power value for network construction by calculating the scale-free topology fit index for a set of candidate powers, ranging from 1 to 30. In this way, the appropriate power was determined when the index value for the reference dataset exceeded 0.8. Once the soft-thresholding power value was set, the WGCNA algorithms were used to construct the co-expression modules. A module was defined as a group of highly interconnected genes (30). The minimum number of genes for each module was set at 30. Co-expression networks or modules were defined as branches of a hierarchical clustering tree and each module was assigned a unique color label.

6. Identification of gene modules associated with BMD Z score in childhood asthmatics

The module eigengene is defined as the first principal component of a given module. It can be considered representative of the gene expression profiles in a module. We computed the eigengene values of the identified modules and performed multivariate linear regression analysis adjusted for baseline age, gender, BMD Z score, vitamin D level, Tanner stage, and body mass index Z score. Eigengene values can be effective and biologically meaningful tools for studying the relationships between modules of a gene co-expression network

and phenotypes (31). The BMD Z score-associated common module was defined when its eigengene value was significantly associated with the BMD Z score, a target phenotype.

7. Replication of the BMD Z score-associated common module in adult asthmatics

Next, we tested if the BMD Z score-associated common module identified in childhood asthmatics was preserved in gene expression profiles from adult asthmatics using the R package "NetRep" (32). Replication was assessed in two ways: preservation of a module (the consistency of the network module structure across gene expression profiles) and preservation of association (association between corresponding eigengene values and the BMD Z score). NetRep can quantify the preservation of gene co-expression modules across different datasets and produce unbiased p values based on a permutation approach to score module preservation without assuming data are normally distributed (32). The BMD Z score-associated common module signified a module that was identified in gene expression profiles from childhood asthmatics and was significantly preserved in gene expression profiles from adult asthmatics. We then calculated the eigengene value of the BMD Z score-associated common module in adult asthmatics and performed multivariate

linear regression analysis adjusted for age, gender, vitamin D level, body mass index, and smoking status.

8. Preservation of the common gene module in osteoblast gene expression

As PBMCs and IBCs are not directly involved in bone metabolism, we searched for relevance of the identified common gene module in the target tissue of BMD. For this purpose, a public gene expression dataset of sham-treated osteoblasts (GSE21727) (33) was used. This dataset was generated from cultured trabecular bone cells obtained from ~100 unrelated Caucasian donors.

9. Gene set enrichment analysis of genes belonging to the BMD Z score-associated common module

To assign biological meaning to the interpretability of the BMD Z score-associated common module, pathway enrichment analyses in Gene Ontology (GO) biological process categories were performed using its membership genes. The author performed GO pathway overrepresentation analyses of the BMD Z score-associated common module using “g:Profiler” (database version: r1730_e88_eg35) (34). g:Profiler (https://biit.cs.ut.ee/gprofiler/) provides an adjusted P value calculated in a manner that accounts for the hierarchical

relationships among the tested gene sets. To increase the specificity of the enrichment results, a more stringent threshold of overlap (intersection of query and test sets $\geq$ 3) was set. *P* values of less than or equal to 0.05 after correction were considered statistically significant.

10. Functional replication of identified biological pathways in another genomics dataset

The relevance of the identified enriched pathways was tested again in another genomics dataset. We used the results of a genome-wide association study of 489 children with asthma, including those enrolled in this study. (7) The purpose of this study was to identify genetic factors influencing oral corticosteroid dose effects on bone mineral accretion in children with asthma. A pathway analysis was performed using the top-200 SNPs (Table 1) that were significantly associated with bone mineral accretion.

11. Identification of hub genes in the BMD Z score-associated common module

As the occurrence of certain diseases is less likely to be associated with abnormalities in the whole set of genes involved in the biological pathway, we searched for the key driving hub genes in the BMD Z score-associated common

module. Hub genes were defined by module connectivity, measured by the absolute value of the Pearson's correlation coefficient (cor.geneModuleMembership > 0.8) and clinical trait relationship, measured by the absolute value of the Pearson's correlation coefficient (cor.geneTraitSignificance > 0.2) (14, 30). For the pathway analysis of SNPs, we selected the top-200 SNPs from our previous report (7) and ran these SNPs through ICSNPathway (http://icsnpathway.psych.ac.cn/). The ICSNPathway web server enabled us to identify candidate causal SNPs and pathways from a genome-wide association study using one analytical framework (35). The following parameters were used: SNP, P value < 1.0E-5; linkage disequilibrium cutoff, r^2=0.8; rule of mapping SNPs to genes, within gene; population, CEU; Pathway gene set size, minimum=5 and maximum=100; FDR cutoff, 0.05.

12. *In vitro* perturbations of the co-expression modules

Gene expression profiling of *in vitro* drug perturbations is useful for many biomedical discovery applications. To evaluate *in vitro* perturbations of identified modules identified, we observed changes in the module structure between sham- and Dex-treated IBCs. IBCs derived from childhood asthmatics were cultured in RPMI 1640 medium (sham-treated IBCs) and treated with dexamethasone (10^{-6} M) for 6 hours (Dex-treated IBCs).

13. Statistical analysis

Statistical analysis was performed using R version 3.4.3 (www.r-project.org). We performed WGCNA on each gene expression profile using the R package "WGCNA" (30) to identify cluster modules of highly correlated genes. Multivariate linear repression analysis was performed to evaluate the module-BMD score relationship. All P values were two-sided and P value < 0.05 was considered significant.

Results

1. Subject Characteristics

The clinical characteristics of the subjects in this study are presented in Table 2. A total of 32 childhood asthmatics whose IBCs and BMD profiles were available and 17 adult asthmatics were included. In childhood asthmatics, 72% of the subjects were male, compared to 35% in adult asthmatics. The mean age of subjects was 8.63 years in childhood asthmatics and 60.11 years in adult asthmatics. The mean baseline vitamin D level was 31.81 ng/mL in childhood asthmatics and 14.71 ng/mL in adult asthmatics.

2. Identifying co-expression gene modules and evaluation of BMD Z score association in childhood asthmatics

By applying WGCNA to the 5,000 genes expressed in sham-treated IBCs, we identified 10 co-expression modules of various sizes ranging from 125 genes in the purple module to 1,372 genes in the turquoise module (Figure 2). To emphasize the impact of strong correlations over weak ones in the network construction, we chose an empirical soft threshold of 6, representing a strong model fit for scale-free topology ($R^2 > 0.8$, Figure 3). A total of 63 genes could not be assigned to any module as a membership gene, and were grouped into

the gray module, which was not considered for further analysis. Eigengene values of two modules (blue and magenta modules) showed significant associations with the BMD Z score in multivariate linear regression analysis. Eigengene value of the blue module consisting of 794 genes was negatively associated with the BMD Z score (P = 0.00294), whereas that of the magenta module containing 199 genes showed a positive association (P = 0.000758) (Figure 4).

3. Replication of BMD Z score-associated common module in adult asthmatics

Among the 10 modules identified in the discovery cohort, three modules (turquoise, magenta, and purple modules) were significantly preserved in the replication cohort (Figure 5). Module preservation statistics and P values are presented in Table 3. Multivariate linear regression analysis showed that the eigengene value of the magenta module was also significantly associated with the BMD Z score in the replication cohort (P = 0.0104) (Figure 6). Based on these findings, we labeled the magenta module identified in gene expression profiles from childhood asthmatics as the BMD Z score-associated common module.

4. Preservation of BMD Z score-associated common

module in osteoblast gene expression dataset

The magenta module identified in this study was preserved in gene expression of sham-treated osteoblasts (a maximal permutation P = 0.0000599; Table 4 and Figure 7). This module was not preserved in gene expressions of Dex-treated osteoblasts (a maximal permutation P = 0.253; Data not shown).

5. Gene set enrichment analysis of genes in the BMD Z score-associated common module

The most significantly enriched pathway was the cellular metabolic pathway (GO:0044237, FDR adjusted P value = 2.75E-7). This pathway consists of 10,751 genes, with an overlap of 150 genes out of the 199 genes belonging to the BMD Z score-associated common module. Identified enriched pathways are shown in Table 5.

6. Functional replication of identified biological pathways

A pathway analysis using genes mapped to the 200 SNPs that have been associated with bone mineral accretion in another genomic data, identified the cellular macromolecular metabolic process (GO:0044260) as the most

significant candidate causal pathway (FDR P value = 0.02).

7. Identification of hub genes in the BMD Z score-associated common module

Among the 199 membership genes in the BMD Z score-associated common module, 18 genes (*ARMC5, ATP2A2, CCNK, CREBBP, EP300, EP400, GTF3C1, IPO13, MTF1, NOL8, NUP188, PCF11, RFX5, SDAD1, SETD1A, SLC25A22, UBAP2L, WDR59*) were selected as hub genes due to their high connectivity and association with the BMD Z score (Figure 8 and Table 6).

8. *in vitro* perturbation of BMD Z score-associated common module

Among the 10 modules, only the magenta module identified in Sham-treated IBCs was not preserved in Dex-treated IBCs (a maximal permutation P = 0.096, Table 7). Additionally, a co-expression network of the 18 hub genes showed distinct differences in their connections (Figure 9).

Discussion

The purpose of this study was to identify key biological pathways associated with glucocorticoid-induced BMD derangement, including a reduction in bone mineral accretion in childhood asthmatics and a reduction in BMD in adult asthmatics after long-term treatment with glucocorticoids. WGCNA enables identification of the correlation and topology between genes or proteins, and clustered genes (a gene co-expression module) reflect the biological processes of the diseases more comprehensively than single gene/protein analysis. Using gene expression profiles on blood cells, we identified a key gene module composed of 199 genes whose eigengene value showed a significant association with the BMD Z score in both, childhood and adult asthmatics and whose connectivity was preserved as well.

Membership genes in this module were significantly overrepresented in the cellular metabolic pathway (GO:0044237). This GO pathway is consistent with the findings of a previously published study. A previous report exploring differential gene expression profiles of PBMCs using the graph clustering approach and GO term enrichment analysis showed 9 gene clusters associated with osteoporosis (36). These 9 clusters included various GO pathways, such as response to virus (GO:0009615), immune response (GO:0006955), response to hypoxia (GO:0001666), and response to extracellular stimulus (GO:0009991) that were similar to the GO pathways identified in this study. The cellular

metabolic pathway representing the chemical reactions and pathways by which individual cells transform chemical substances have never been recognized in previous studies focused on osteoporosis.

To obtain further insight, we performed a pathway analysis using the genes mapped to the top-200 SNPs that were significantly associated with bone mineral accretion in childhood asthmatics in our previous genome-wide association study (7). We identified the cellular macromolecular metabolic process (GO:0044260) as the most important candidate causal pathway. This pathway is a sub-pathway of the cellular metabolic pathway (GO:0044237) (37). These SNPs could not be directly linked to gene expression/modules identified in the present study, as genomics data were generated from different populations. However, we believe that this result would provide additional information suggesting a possible role of the cellular metabolic pathway in osteoporosis pathogenesis. Cellular metabolism is an important part of bone biology and homeostasis (38, 39). However, to date, no direct evidence connecting this pathway to glucocorticoid-induced BMD derangement has been presented, although the cellular amine metabolic pathway (GO:0033240)) – a sub-pathway of the cellular metabolic pathway) – was reported to be enriched in gene expressions profiles of PBMCs from patients with osteoporosis compared to those from normal people (22). Further studies are needed to confirm our observations.

It was challenging to assign biological meanings to our findings at the pathway level, as the identified pathways were diverse and contained many genes (for example, the cellular metabolic pathway included 9416 genes) (37). For this reason, we selected 18 highly connected intramodular hub genes. By reviewing available literature, we selected two genes of putative interest: *EP300* encoding E1A binding protein p300 and *CREBBP* coding CREB binding protein (CBP). CBP and p300 are highly related transcriptional co-activators possessing histone acetyltransferase activity and are known to participate in the activities of hundreds of different transcription factors involved in a variety of cell functions (40). Upregulation of miR-132-3p could partly inhibit osteoblast differentiation by decreasing p300 expression (41), and CBP could mediate osteoblast-adipocyte lineage plasticity by interacting with Maf (42, 43). Additionally, both CBP and p300 are known to be important co-factors mediating transforming growth factor-beta and bone morphogenic protein signaling, which have fundamental roles in bone homeostasis (44), and to modulate parathyroid hormone regulation of osteoblasts (45). Interestingly, it has also been also reported that these two proteins are involved in steroid receptor signaling (46). Steroid receptors require co-activators for efficient activation of target gene expression, and these co-activators might contribute towards tissue-specific responses to steroid hormones. Likewise, CBP and p300 might function in tandem or antagonistically to each other depending on their

relative concentrations and type of target tissue, to influence the sensitivity of tissues to glucocorticoids (47). Furthermore, it has been reported that *CREBBP* mutations result in impaired expression of GC receptor-responsive genes and impaired histone acetylation and transcriptional regulation (48, 49). Given that CBP and p300 are involved not only in bone homeostasis but also in glucocorticoid receptor signaling, our study is significant because a gene module containing *CREBBP* and *EP300* may play an important role in glucocorticoid-induced derangement in BMD.

Among other genes belonging to the hub genes, *ARMC5* encoding armadillo repeat containing 5 and *IPO13* encoding importin 13 are of interest. *ARMC5* inactivation affects steroid production and cell survival *in vitro* and causes adrenal hyperplasia associated with severe Cushing's syndrome (50). As is well known, Cushing's syndrome results in osteoporosis that is analogous to glucocorticoid-induced osteoporosis (51). *IPO13* is a steroid-inducible gene, and the glucocorticoid receptor is a cargo substrate for importin 13 (52). *IPO13* is thus possibly associated with glucocorticoid signaling, although its role in glucocorticoid-induced osteoporosis is unknown.

Differences in the expression of 18 hub genes of a gene module discovered in this study according to the BMD Z score were analyzed. In pediatric asthma patients, the expression of *ARMC5* and *SDAD1* was significantly lower in the lower-BMD Z score group than in the upper-BMD Z score group ($p = 0.050$ and 0.022, respectively). The lower-BMD Z score group showed lower levels

of *ARMC5* expression (p = 0.050) and higher levels of *ATP2A2* expression (p = 0.007) than those in the upper-BMD Z score group in adult asthmatics. Additionally, subgroup analysis according to gender was performed, as hormonal changes can affect BMD in middle-aged or elderly patients. There was no difference in hub gene expressions based on gender.

The strength of our study was that we searched biological mechanisms underlying glucocorticoid-induced derangement in BMD with a network based methodology for the first time. A recent review highlighted an importance of network-based approach in genomic studies for osteoporosis (53). Considering that the modularity of networks is inherent to cell biology and thus molecular interactions organized into functional unit are more relevant to explain biological phenomena (13), the present study might provide a comprehensive and holistic understanding of glucocorticoid-induced derangement in BMD. To generate biological networks, we utilized WGCNA in the present study. WGCNA, unlike the other biological networks, is a way to organize data in an unbiased manner and provides a gene module summary which can be related with clinical phenotypes (53). In a systems genetics aspect, if a Bayesian structure learning algorithm is to be applied to WGNCA, the direction of the flow of molecular information would be elucidated, which enables us figure out the causal relationship. Recently, such an attempt identified novel pathways in patients with the late-onset Alzheimer's disease pathology and coronary artery disease (54, 55). However, to our knowledge, Bayesian structure learning

algorithm in WGNCA has not yet been applied in the field of bone mineral density and steroid response. Another important thing is that we can analyze co-expressions across a set of perturbations with WGCNA. In the present study, we found that a structure of the BMD Z score-associated common module was disrupted by *in vitro* perturbation using gene expression profiles of Dex-treated IBCs. Eigengene values of this module showed significant positive associations with the BMD Z score in both childhood and adult asthmatic (Figure 6). We assume that a disruption of this protective gene module by glucocorticoid may result in BMD reduction in asthmatics treated by glucocorticoid for a long time, which provides a functional relevance of our observations. In addition, we confirmed that a module significantly associated with the BMD Z score preserved in different conditions (bone mineral accretion in childhood asthmatics and osteoporosis in adult asthmatics), which may increase the generalizability of observations in this study.

There are some limitations in our study. First, we utilized gene expression profiles of blood cells instead of cells directly involved in bone biology. Peripheral blood is an easily accessible tissue and it was suggested that molecular profiling of peripheral blood might reflect physiological and pathological events occurring in different tissue of the body (56). Especially, human peripheral blood monocytes serve as precursors of osteoclasts and produce cytokines regulating differentiation, activation, and apoptosis of osteoclast (57), and they have already been established as a well working cell

model for studying gene/protein expression patterns in regard to osteoporosis (58-61). Moreover, recent reports showed that PBMCs could be used to assess glucocorticoid sensitivity or efficacy of osteoporosis treatment (62, 63). To overcome the limitation of this study using only peripheral blood cells, we used a publicly available gene expression dataset of Sham- and Dex-treated osteoblast (GSE21727) (33) and the magenta module was preserved in gene expressions of Sham-treated osteoblasts. These findings suggested that a gene modules of this study might be important across different tissue types (blood cells and osteoblast), although GSE21727 was a small dataset (one subject with three replicates). Evidently, previous reports showed that tissue-specific genes can be expressed in non-tissue-specific manner (64, 65), and peripheral blood cells expressed approximately over 80% of the genes encoded by the human genome (66). In addition, it was demonstrated that osteoclasts could be generated from PBMC population (67, 68) and PBMC could be used to assess efficacy of osteoporosis treatment (62). Taken together, peripheral blood cells may be a surrogate for bone tissue and recapitulate bone cell biology in part, although further studies will be needed. Secondly, some characteristics (ethnicity, age, and accumulative dose of corticosteroids) of replication data set for validation were different from the discovery data set. Previously, age-dependent alterations in osteoblast and osteoclast activity were reported (69, 70). In general, short-term glucocorticoid use was associated with mild adverse effects, whereas long-term use might be associated with more serious sequel

including osteoporosis (71). For this reason, we provided information on the hub genes and enriched biologic pathways of genes belong to the blue module, a childhood asthmatics-specific gene module, in the supplementary information (Figure 10, Table 8, and Table 9). Currently, there are no publicly available datasets to validate our findings. However, a replication analysis should be done when datasets become available. Finally, a small number of participants is another weakness of this study and an integrative analysis using other potentially relevant -omics data such as, miRNAs, lncRNAs, and methylation profiles is warranted in the future.

In conclusion, the potentially significant genes and pathways identified in our analysis may help further elucidate of the molecular mechanisms and provide novel insights regarding glucocorticoid-induced derangement in BMD in asthmatics.

Table 1. The top-200 SNPs obtained from previous GWAS study

rs7003550	rs9473350	rs236113	rs764251	rs2346008	rs9817986
rs9896933	rs1911254	rs869697	rs9647406	rs1369351	rs4779618
rs7599706	rs7822757	rs11149155	rs12232191	rs2273866	rs4877971
rs12447718	rs6602747	rs1209633	rs4786860	rs17040590	rs10812520
rs4368243	rs739994	rs1376478	rs966935	rs9831609	rs1782322
rs2316527	rs770236	rs4837698	rs1028458	rs2824280	rs10801804
rs4484658	rs4853475	rs2840945	rs2386983	rs7212240	rs4495950
rs7506840	rs1367685	rs4945688	rs6845304	rs1208209	rs10464035
rs10485681	rs1896950	rs10926977	rs10514688	rs6428587	rs17217760
rs3756612	rs4886620	rs226313	rs9915334	rs2825560	rs1040151
rs12149765	rs1903876	rs10511185	rs7176566	rs939533	rs675566
rs10251582	rs8074277	rs2048920	rs6771233	rs12101676	rs2182954
rs2275732	rs2117906	rs9341793	rs2824317	rs4957696	rs6963373
rs7818862	rs3743487	rs4913287	rs1239104	rs7587023	rs1126328
rs12287409	rs7149088	rs2572283	rs2401035	rs10841528	rs220611
rs7930174	rs998235	rs7139901	rs1394551	rs8111710	rs10778889
rs962963	rs11058317	rs1945503	rs10257931	rs17608067	rs10791993
rs2187331	rs1011692	rs12118850	rs12432642	rs6758317	rs2001558
rs17678758	rs7154679	rs4677414	rs236111	rs6591350	rs3810524
rs6678151	rs2341459	rs6493265	rs11252485	rs4480073	rs2030737
rs303006	rs1105274	rs16940375	rs9856875	rs6500586	rs10087773
rs6951422	rs6023633	rs3745788	rs1469572	rs242412	rs7835456
rs1550948	rs6957858	rs9572552	rs281505	rs136070	rs10494229
rs220612	rs4864471	rs12539392	rs1462831	rs17014050	rs6130139
rs1494023	rs12639326	rs2099613	rs2146880	rs17094058	rs2930796
rs7689090	rs2007888	rs386790	rs4420519	rs1956108	rs16983718
rs715693	rs4336567	rs10243420	rs2281169	rs6772123	rs2930796
rs242405	rs2436634	rs242401	rs17153785	rs12918809	rs2073831
rs6930328	rs2814848	rs12740041	rs889104	rs2825544	rs2144800
rs763853	rs1996709	rs7097254	rs2347935	rs7166898	rs1438182
rs6572555	rs1385432	rs12520537	rs11242598	rs12880735	rs7403455

rs10262486	rs1468627	rs17015512	rs1949929	rs11700399	rs9888659
rs303000	rs10801805	rs2825581	rs2732231	rs1927731	rs1435218
rs4143188	rs12232511				

Table 2. Characteristics of subjects enrolled

	Childhood asthmatics[†] (n = 32)	Adult asthmatics[‡] (n = 17)
Gender, male (%)	23 (71.9)	6 (35.3)
Age, year	8.63 (1.93)	60.11 (11.71)
Smoking, yes (%)	Not applicable	3 (17.65)
Body mass index, kg/m^2	17.71 (3.21)	23.72 (5.18)
Vitamin D, ng/mL	31.81 (9.97)	14.71 (7.72)
Tanner stage (%)		
I/II/III/IV/V	24 (75.0)/6 (18.8)/1(3.1)/1 (3.1)	Not applicable
Baseline BMD Z-score	-0.10 (2.23)	Not available
Ethnicity (%)		
Non-Hispanic white	32 (100)	0
Asian	0	17 (100)
Cumulative dose of PD, mg	1188.40 (608.05)	3130.53 (1552.09)
Final BMD Z-score	-0.29 (0.81)	-0.97 (1.37)

Data indicate mean (Standard deviation); BMD, Bone mineral density; PD, Prednisone; [†]Characteristics measured at enrollment of the CAMP study except cumulative dose of prednisone and the final BMD Z-score; [‡]Characteristics measured at enrollment of the present study

Table 3. Preservation statistics and P values of modules identified in gene expression profiles of Sham-treated immortalized B cells from childhood asthmatics in gene expression profiles of Sham-treated peripheral mononuclear cell from adult asthmatics

	Module	avg.weight	coherence	cor.cor	cor.degree	cor.contrib	avg.cor	avg.contrib
Statistics	Turquoise	0.3189273	0.2815515	0.1016 7908	0.2329 22271	0.30219 3872	0.0233 12781	0.1308 60688
	Magenta	0.3019563	0.2635123	0.1701 0856	0.1843 81214	0.37269 7861	0.0940 3571	0.3168 96154
	Purple	0.2611963	0.2256738	-0.0286 8263	0.0214 43337	-0.18841 6992	0.0084 46526	0.0559 97275
P values	Turquoise	0.0000 9999	0.0004 9995	0.0000 9999	0.0000 9999	0.00009 999	0.0000 9999	0.0000 9999
	Magenta	0.0000 9999	0.0000 9999	0.0000 9999	0.0059 994	0.00009 999	0.0000 9999	0.0000 9999
	Purple	0.0021 9978	0.0000 9999	0.0000 9999	0.0000 9999	0.00009 999	0.0000 9999	0.0000 9999

Columns correspond to seven module preservation statistics defined by the “NetRep” package and P values are permutation P values.
'avg.weight' measures the average magnitude of edge weights in the test dataset, that is, how connected nodes in the module are to each other on average.

'coherence' measures the proportion of variance in the module data explained by the module's summary profile vector in the test dataset.

Table 4. Preservation statistics and P values of modules identified in gene expression profiles of Sham-treated immortalized B cells in gene expression profiles of Sham-treated osteoblast from GSE21727

	Module	avg.weight	coherence	cor.cor	cor.degree	cor.contrib	avg.cor	avg.contrib
Statistics	Turquoise	0.6544096	0.6031521	0.04222102	0.1172 34467	0.1278 2118	0.0124 55046	0.0898 8802
	Blue	0.6514467	0.5967116	0.03307033	0.0463 51508	0.1110 2283	0.0192 90233	0.1155 0161
	Brown	0.6537856	0.603804	0.03447525	0.0071 0907	0.0609 9031	0.0176 51138	0.0626 3249
	Yellow	0.6799488	0.6645311	0.46249519	0.3002 56852	0.7350 7939	0.3192 78805	0.5757 4776
	Green	0.6822337	0.6677667	0.3033763	0.2539 27274	0.4940 0758	0.2492 50918	0.5055 1534
	Red	0.6781878	0.6600332	0.32291358	0.0865 56734	-0.6299 1583	-0.2127 33097	-0.4503 2814
	Black	0.6460818	0.5811741	0.01554291	0.0712 96112	0.0428 7394	0.0087 92729	0.0678 776
	Pink	0.6525093	0.6015149	0.04848967	0.0071 40164	0.1907 9314	0.0235 72609	0.1516 882

	Magenta	0.6917683	0.6869658	0.29738041	0.32694967	0.47228733	0.23880409	0.4903798
	Purple	0.7006673	0.7004956	0.28914427	0.26406210	0.41262065	0.35040914	0.5913968
P values	Turquoise	0.6520348	0.7048295	0.00009999	0.00009999	0.00009999	0.00009999	0.00089991
	Blue	0.8453154	0.8381161	0.00009999	0.09829017	0.0009999	0.00009999	0.00049995
	Brown	0.6397360	0.6307369	0.00009999	0.4279572	0.06079392	0.00009999	0.02569743
	Yellow	0.0002 9997	0.0002 9997	0.0000 9999	0.0000 9999	0.0000 9999	0.0000 9999	0.0000 9999
	Green	0.0003 9996	0.0002 9997	0.0000 9999	0.0000 9999	0.0000 9999	0.0000 9999	0.0000 9999
	Red	0.0008 9991	0.0011 9988	0.0000 9999	0.0489951	1	0.0000 9999	1
	Black	0.9308 0692	0.9289 0711	0.0144 9855	0.1050 8949	0.2279772	0.0295 9704	0.1023 8976
	Pink	0.6138 3862	0.6401 3599	0.0005 9994	0.4660 5339	0.0019998	0.0044 9955	0.0055 9944
	Magenta	0.0005 9994	0.0003 9996	0.0000 9999	0.0000 9999	0.0000 9999	0.0000 9999	0.0000 9999

Purple	0.0020 9979	0.0017 9982	0.0000 9999	0.0013 9986	0.0000 9999	0.0000 9999	0.0000 9999

Table 5. Biological pathways enriched in the bone mineral density Z score-associated common module

ID	Name†	Depth‡	P value§
GO:1903901	Negative regulation of viral life cycle	1	0.0418
GO:0045071	Negative regulation of viral genome replication	1	0.014
GO:0006475	Internal protein amino acid acetylation	1	0.0448
GO:0018394	Peptidyl-lysine acetylation	1	0.0453
GO:0018393	Internal peptidyl-lysine acetylation	2	0.0394
GO:0018076	N-terminal peptidyl-lysine acetylation	2	0.0287
GO:0016570	Histone modification	1	0.0291
GO:0016573	Histone acetylation	2	0.0352
GO:0010646	Regulation of cell communication	1	0.0485
GO:0051169	Nuclear transport	1	0.041
GO:0006913	Nucleocytoplasmic transport	2	0.0374
GO:0002886	Regulation of myeloid leukocyte mediated immunity	1	0.0321
GO:0002279	Mast cell activation involved in immune response	1	0.0453
GO:0051640	Organelle localization	1	0.0335
GO:0043300	Regulation of leukocyte degranulation	1	0.0336

	Establishment of organelle		
GO:0051656	localization	1	0.0052
GO:0033003	Regulation of mast cell activation	1	0.0283
	Regulation of mast cell activation involved in immune		
GO:0033006	response	2	0.0153
GO:0043303	Mast cell degranulation	1	0.0453
	Regulation of mast cell		
GO:0043304	degranulation	2	0.0153
GO:0050657	Nucleic acid transport	1	0.0335
GO:0051236	Establishment of RNA localization	1	0.0354
GO:0050658	RNA transport	2	0.0335
GO:0006405	RNA export from nucleus	3	0.0287
	Ribonucleoprotein complex		
GO:0071166	localization	1	0.0219
	Ribonucleoprotein complex		
GO:0071426	export from nucleus	2	0.0205
GO:0008150	Biological process	1	0.0023
	Cellular component		
GO:0071840	organization or biogenesis	2	0.0279
	Cellular component		
GO:0044085	biogenesis	3	0.001
			0.000002
GO:0008152	Metabolic process	2	88
GO:0044238	Primary metabolic process	3	0.000013
	Organic substance metabolic		0.000018
GO:0071704	process	3	8
GO:0009058	Biosynthetic process	3	0.000516

	Nitrogen compound		0.000027
GO:0006807	metabolic process	3	3
GO:0009987	Cellular process	2	0.000425
			0.000000
GO:0044237	Cellular metabolic process	3	275
	Macromolecular complex subunit		
GO:0043933	organization	1	0.0278
	Protein complex subunit		
GO:0071822	organization	2	0.019
GO:0065003	Macromolecular complex assembly	1	0.0289
GO:0006461	Protein complex assembly	2	0.0278
	Negative regulation of gene		
GO:0010629	expression	1	0.0138
	Negative regulation of transcription		
GO:0000122	from RNA polymerase II promoter	1	0.0272
GO:0002520	Immune system development	1	0.0138
	Hematopoietic or lymphoid		
GO:0048534	organ development	2	0.0167
GO:0030097	Hemopoiesis	3	0.0225
GO:0006325	Chromatin organization	1	0.034
GO:0031648	Protein destabilization	1	0.0356
GO:0033554	Cellular response to stress	1	0.00328
	Cellular response to decreased		
GO:0036294	oxygen levels	1	0.0448
GO:0071456	Cellular response to hypoxia	2	0.038
	Regulation of transcription from		
	RNA polymerase II promoter in		
GO:0043618	response to stress	1	0.0428

	Regulation of transcription from RNA polymerase II promoter in		
GO:0061418	response to hypoxia	2	0.0466
GO:0051649	Establishment of localization in cell	1	0.0302

[†]Gene ontology biological pathway, [‡]Only depth 1 ~ 3 were presented,

[§]Benjamini-Hocherg FDR P value

Table 6. Hub genes of the bone mineral density Z score-associated common module

Gene	Dexamethasone-responsiveness[†]		Cellular metabolic process gene[‡]
	log2 fold change	P value	
ARMC5	-0.0380249	0.5828633	No
ATP2A2	0.4167439	0.004790925	No
CCNK	-0.03142452	0.8246246	Yes
CREBBP	0.3673004	0.01933958	Yes
EP300	0.1895247	0.04375724	Yes
EP400	0.08339024	0.4198441	Yes
GTF3C1	-0.09396902	0.3400058	Yes
IPO13	-0.216802	0.03394458	Yes
MTF1	0.09902032	0.2934905	Yes
NOL8	0.4393377	0.004976667	Yes
NUP188	0.2586276	0.03014498	Yes
PCF11	0.363114	0.01749985	Yes
RFX5	-0.7230053	4.46E-05	Yes
SDAD1	-0.000207901	0.9989959	No
SETD1A	0.05012735	0.6606172	Yes
SLC25A22	-0.2194058	0.03049449	Yes
UBAP2L	0.07363605	0.6235542	Yes
WDR59	0.2273785	0.1046839	No

[†]Results from GSE21727, [‡]Enriched pathway identified in this study

Table 7. Preservation statistics and P values of modules identified in gene expression profiles of Sham-treated immortalized B cells in gene expression profiles of Dex-treated immortalized B cells from childhood asthmatics

	Module	avg.weight	coherence	cor.cor	cor.degree	cor.contrib	avg.cor	avg.contrib
Statistics	Turquoise	0.04480772	0.3939333	0.9084948	0.9362422	0.9700504	0.3305905	0.569255
	Blue	0.01745769	0.2799837	0.8738084	0.9297415	0.9748477	0.2421161	0.4773045
	Brown	0.0190389	0.2947596	0.8656649	0.8930164	0.9594337	0.2497806	0.4839285
	Yellow	0.03345755	0.384043	0.8976904	0.8185916	0.9632477	0.3312046	0.5726935
	Green	0.03303415	0.3537517	0.869299	0.8185485	0.9455638	0.3061676	0.5390105
	Red	0.0209518	0.3138139	0.8614475	0.779286	0.9602717	0.2765148	0.5203651
	Black	0.02336877	0.327688	0.9012397	0.8693276	0.9762253	0.2929021	0.5329678
	Pink	0.02503431	0.3321562	0.8715029	0.8392627	0.9657686	0.2952158	0.5396827

	Magenta	0.01338425	0.2549678	0.8052235	0.6810665	0.9514463	0.2283777	0.4711403
	Purple	0.07344489	0.437857	0.8687456	0.9264696	0.9230179	0.3536952	0.5899504
P values	Turquoise	0.00009999	0.00009999	0.00009999	0.00009999	0.00009999	0.00009999	0.00009999
	Blue	0.00009999	0.00009999	0.00009999	0.00009999	0.00009999	0.00009999	0.00009999
	Brown	0.00009999	0.00009999	0.00009999	0.00009999	0.00009999	0.00009999	0.00009999
	Yellow	0.00009999	0.00009999	0.00009999	0.00009999	0.00009999	0.00009999	0.00009999
	Green	0.00009999	0.00009999	0.00009999	0.00009999	0.00009999	0.00009999	0.00009999
	Red	0.00009999	0.00009999	0.00009999	0.00009999	0.00009999	0.00009999	0.00009999
	Black	0.00009999	0.00009999	0.00009999	0.00009999	0.00009999	0.00009999	0.00009999
	Pink	0.00009999	0.00009999	0.00009999	0.00009999	0.00009999	0.00009999	0.00009999
	Magenta	0.09609039	0.00029997	0.00009999	0.00009999	0.00009999	0.00009999	0.00009999

Purple	0.0000 9999	0.0000 9999	0.0000 9999	0.0000 9999	0.0000 9999	0.0000 9999	0.0000 9999

Table 8. Hub genes of the blue module (childhood asthmatics-specific gene module)

Gene	Gene	Gene	Gene	Gene
ZDHHC23	RSAD1	CTNNBIP1	TRAK2	SGPP1
TRRAP	PTAFR	SMARCD1	TRIP13	ZNF337
TOB2	POLR2B	RBM15	UBQLN4	CHKA
CELSR3	BLM	CUL1	NT5E	SNRK
LRFN4	PISD	PAQR3	SUPT16H	CCT5
DENND1A	ACAD10	GART	CBFB	SBF1
RAB6A	PIK3R4	RICTOR	KIAA0922	DLL3
RPS6KA5	RNPEPL1	CYLD	MTAP	TTLL12
CSE1L	TRAF5	GPD1L	ABCA3	JSRP1
STAT5B	FBXO21	MYL9	CEBPG	MYO1D
TFAP4	PHF10	TATDN2	ETV6	RNH1
PAK2	BICD2	DCBLD2	ZNF562	
UBE3B	MESDC1	ATP1A1	EXOC6	
TRIM47	RASGRP2	MCM3AP	MCM6	
EML4	TMTC4	RPS6KB1	PSME4	
LMNB2	ETV4	ZNF281	S100A10	
GANAB	ACY3	PRCC	ACOT4	

Table 9. Biological pathways enriched in the blue module (childhood asthmatics-specific gene module)

ID	Name[†]	Depth[‡]	P value[§]
GO:0051348	Negative regulation of transferase activity	1	0.0112
GO:0071705	Nitrogen compound transport	1	0.00577
GO:0033036	Macromolecule localization	1	0.000083
GO:0008104	Protein localization	2	0.0000187
GO:0045184	Establishment of protein localization	3	0.00211
GO:0051641	Cellular localization	1	0.000000237
GO:0070727	Cellular macromolecule localization	2	0.000166
GO:0034613	Cellular protein localization	3	0.000215
GO:0051649	Establishment of localization in cell	1	0.000089
GO:0046907	Intracellular transport	2	0.000269
GO:0035556	Intracellular signal transduction	1	0.0387
GO:0007249	I-kappaB kinase/NF-kappaB signaling	2	0.00979
GO:0043122	Regulation of I-kappaB kinase/NF-kappaB signaling	1	0.00348

GO:0008150	Biological_process	1	5.55E-08
GO:0071840	Cellular component organization or biogenesis	2	0.00000651
GO:0044085	Cellular component biogenesis	3	0.00512
GO:0002376	Immune system process	2	0.000014
GO:0044699	Single-organism process	2	0.00000172
GO:0008152	Metabolic process	2	1.17E-08
GO:0044238	Primary metabolic process	3	0.000000726
GO:0009058	Biosynthetic process	3	0.0151
GO:0009056	Catabolic process	3	0.00000161
GO:0071704	Organic substance metabolic process	3	0.000000274
GO:0006807	Nitrogen compound metabolic process	3	0.0000099
GO:0050896	Response to stimulus	2	0.0025
GO:0042221	Response to chemical	3	0.00178
GO:0009628	Response to abiotic stimulus	3	0.00735
GO:0006950	Response to stress	3	0.00000223

GO:0009607	Response to biotic stimulus	3	0.0176
GO:0006955	Immune response	3	0.00866
GO:0065007	Biological regulation	2	0.000416
GO:0065009	Regulation of molecular function	3	0.00285
GO:0051704	Multi-organism process	2	0.011
GO:0044419	Interspecies interaction between organisms	3	0.0001
GO:0051707	Response to other organism	3	0.00675
GO:0009987	Cellular process	2	1.15E-10
GO:0044763	Single-organism cellular process	3	0.00000227
GO:0016043	Cellular component organization	3	0.0000855
GO:0044237	Cellular metabolic process	3	7.89E-11
GO:0051716	Cellular response to stimulus	3	0.00772
GO:0022402	Cell cycle process	3	0.0000554
GO:0050789	Regulation of biological process	2	0.000326
GO:0050794	Regulation of cellular process	3	0.00472

GO:0019222	Regulation of metabolic process	3	0.000388
GO:0048519	Negative regulation of biological process	2	0.00000102
GO:0048523	Negative regulation of cellular process	3	0.0000874
GO:0009892	Negative regulation of metabolic process	3	0.0114
GO:0048518	Positive regulation of biological process	2	0.00034
GO:0048522	Positive regulation of cellular process	3	0.0372
GO:0002684	Positive regulation of immune system process	3	0.00615
GO:1903320	Regulation of protein modification by small protein conjugation or removal	1	0.000011
GO:1903322	Positive regulation of protein modification by small protein conjugation or removal	2	0.0183
GO:0031396	Regulation of protein ubiquitination	2	0.0000167
GO:0031398	Positive regulation of protein ubiquitination	3	0.0499
GO:0031400	Negative regulation of protein modification process	1	0.0136
GO:1903321	Negative regulation of protein modification by small protein conjugation or removal	2	0.00468
GO:0031397	Negative regulation of protein ubiquitination	3	0.0016
GO:0031349	Positive regulation of defense response	1	0.005

GO:0045089	Positive regulation of innate immune response	2	0.000201
GO:0002218	Activation of innate immune response	3	0.000223
GO:0010243	Response to organonitrogen compound	1	0.0346
GO:0070646	Protein modification by small protein removal	1	0.0202
GO:0016579	Protein deubiquitination	2	0.00678
GO:0051603	Proteolysis involved in cellular protein catabolic process	1	0.00416
GO:0019941	Modification-dependent protein catabolic process	2	0.0045
GO:0006511	Ubiquitin-dependent protein catabolic process	3	0.00729
GO:0002758	Innate immune response-activating signal transduction	1	0.000121
GO:0007159	Leukocyte cell-cell adhesion	1	0.000436
GO:1903037	Regulation of leukocyte cell-cell adhesion	2	0.00417
GO:0050863	Regulation of T cell activation	1	0.00408
GO:2001235	Positive regulation of apoptotic signaling pathway	1	0.0458

†Gene ontology biological pathway, ‡Only depth 1 ~ 3 were presented,

§Benjamini-Hocherg FDR P value

Figure 1. The overall study design

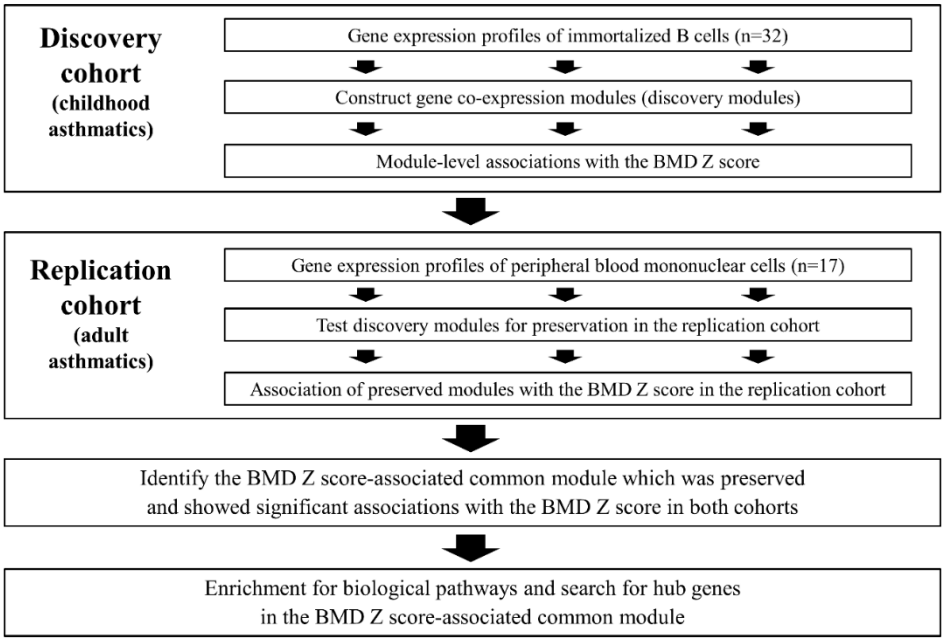

Figure 2. Co-expression modules identified in gene expression profiles of Sham-treated immortalized B cells from childhood asthmatics

Top panel shows a dendrogram of 5,000 genes. Bottom panel shows colors corresponding to the cluster membership labels for each gene.

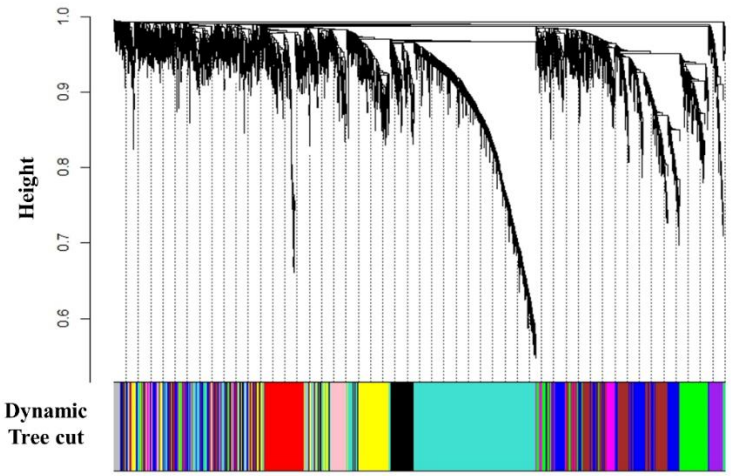

Figure 3. Assessing scale-free model fitting in gene expression profiles Sham-treated immortalized B cells from childhood asthmatics

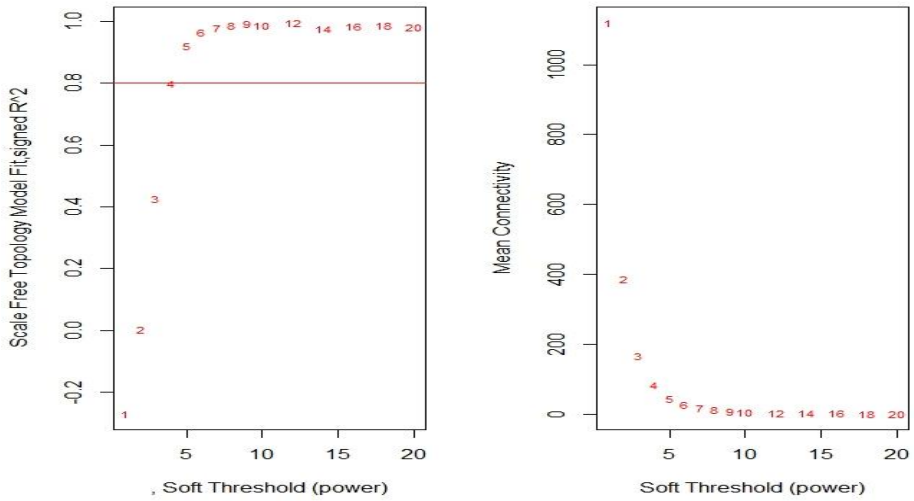

Left panel shows scale-free topology plotted by soft threshold. The left picture displays the scale free fit index (y-axis) as a function of the soft-thresholding power (x-axis). The red horizontal line represents the cutoff for identifying a strong model fit. The right picture shows the mean connectivity (y-axis) as a function of the soft-thresholding power (x-axis).

Figure 4. Correlations between eigengene values of two modules identified in gene expression profiles of Sham-treated immortalized B cells from childhood asthmatics and the bone mineral density Z score

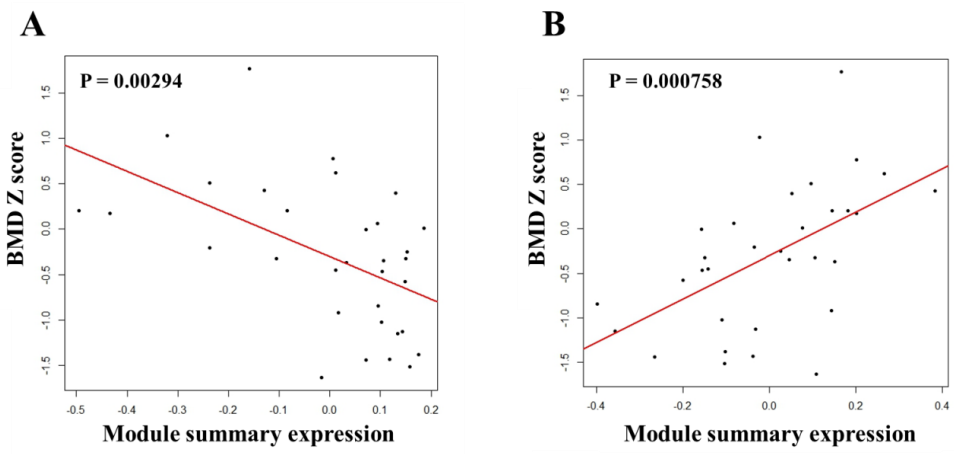

A, Blue gene module; B, Magenta gene module

All P values were adjusted by covariates.

Figure 5. Preservation of modules identified in gene expression profiles of Sham-treated immortalized B cells from childhood asthmatics in gene expression profiles of Sham-treated peripheral mononuclear cell from adult asthmatics

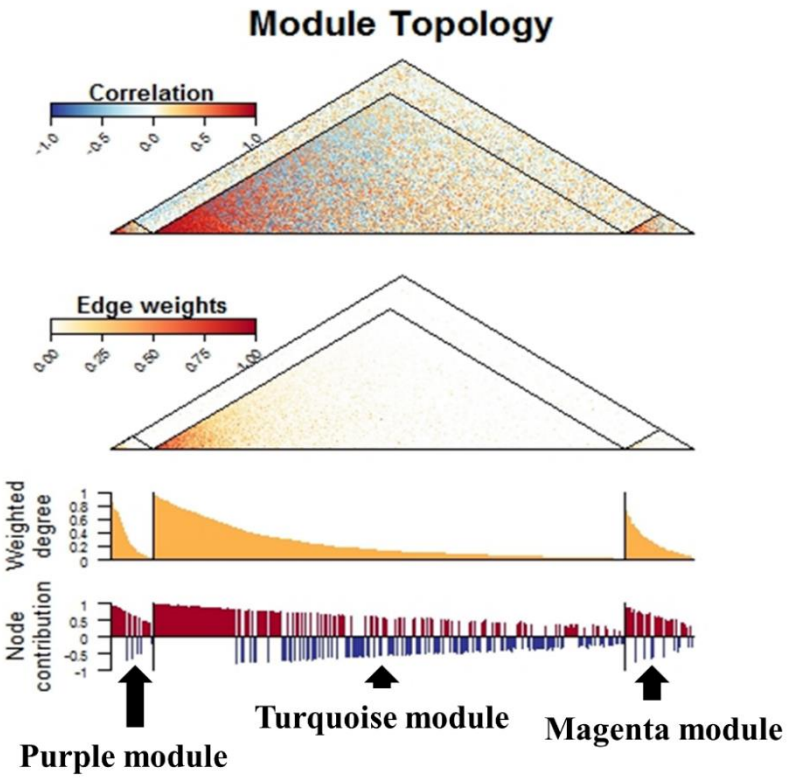

The first (top) panel shows a heatmap of pair-wise correlations among the genes comprising the turquoise, magenta, and purple modules. The second panel shows a heatmap of the edge weights (connections)

among the genes comprising the three modules. The third panel shows the distribution of scaled weight degrees (relative connectedness) among the genes comprising the three modules. The fourth panel shows the distribution of node contributions (correlation to module eigengene) among the genes comprising the three modules. Genes are ordered from left to right based on their weighted degree in the discovery cohort, so as to highlight the consistency of the network properties in the replication cohort.

Figure 6. Associations between eigengene values of the bone mineral density Z score-associated common module (magenta module) and the bone mineral density Z score

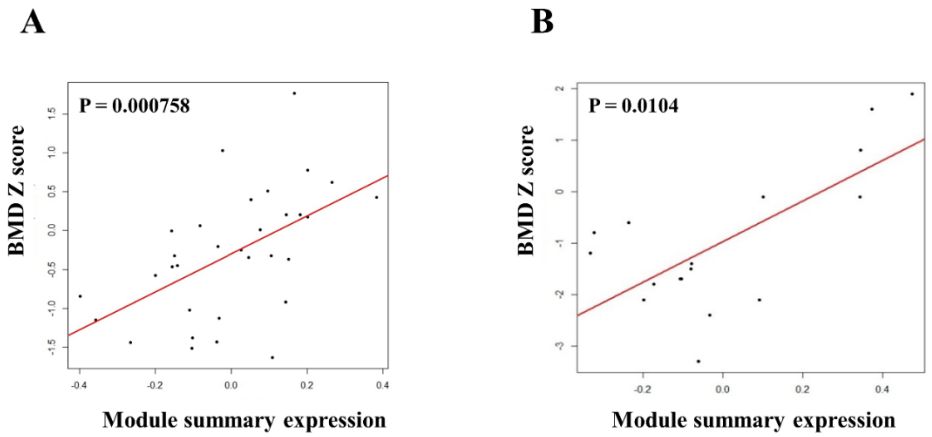

A. Childhood asthmatics

B. Adult asthmatics

Both P values were adjusted by covariates.

Figure 7. Preservation of modules identified in gene expression profiles of Sham-treated immortalized B cells from childhood asthmatics in gene expression profiles of Sham-treated osteoblast from GSE21727

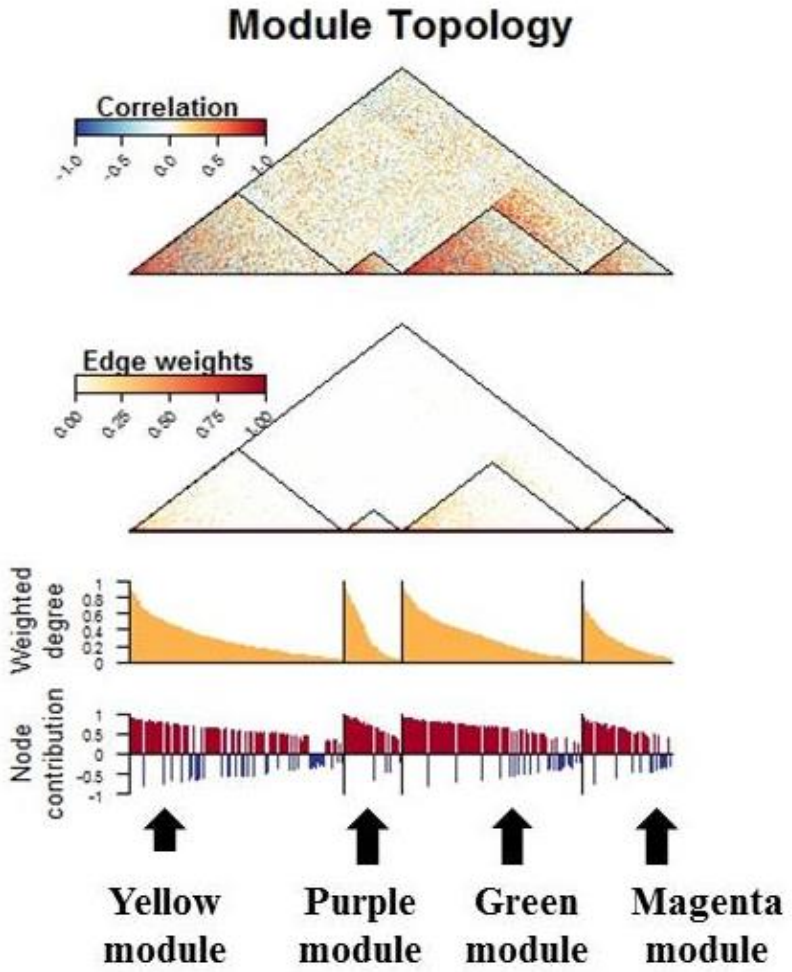

Figure 8. Scatter plot of module eigengenes in the magenta module (bone mineral density Z score-associated common module)

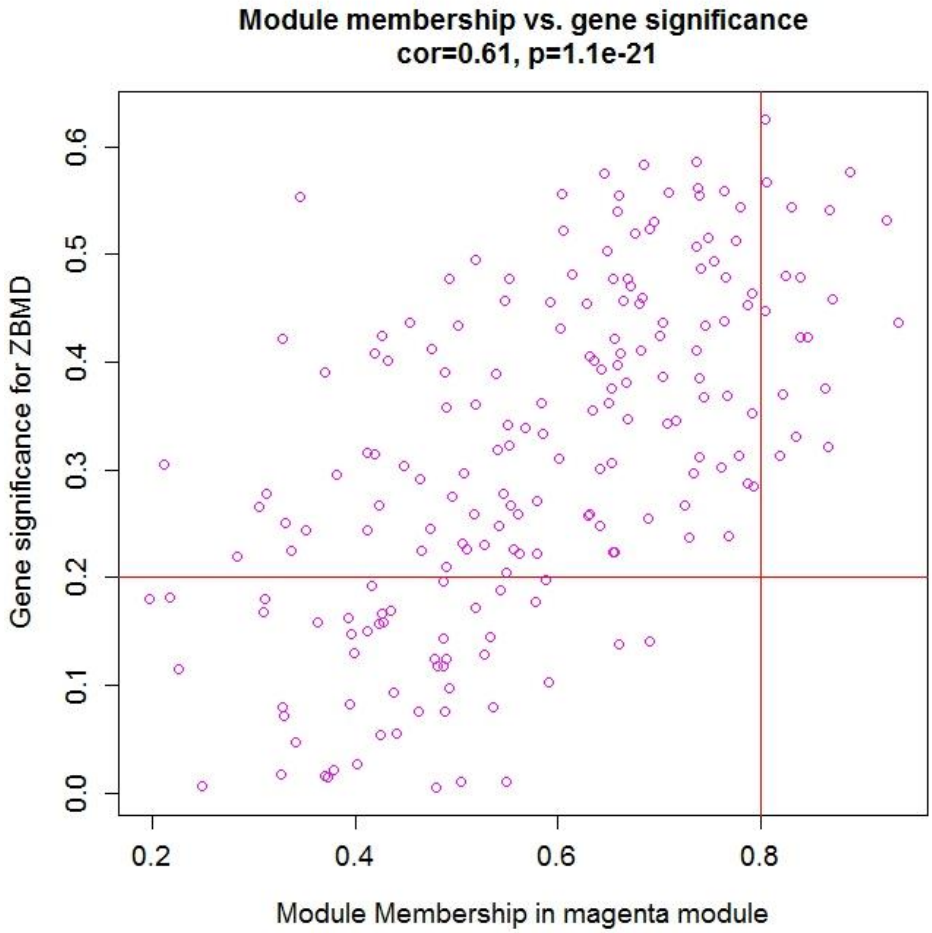

Hub genes are located at the right and upper quadrant.

Figure 9. Co-expression network of hub genes of the bone mineral density Z score-associated common module

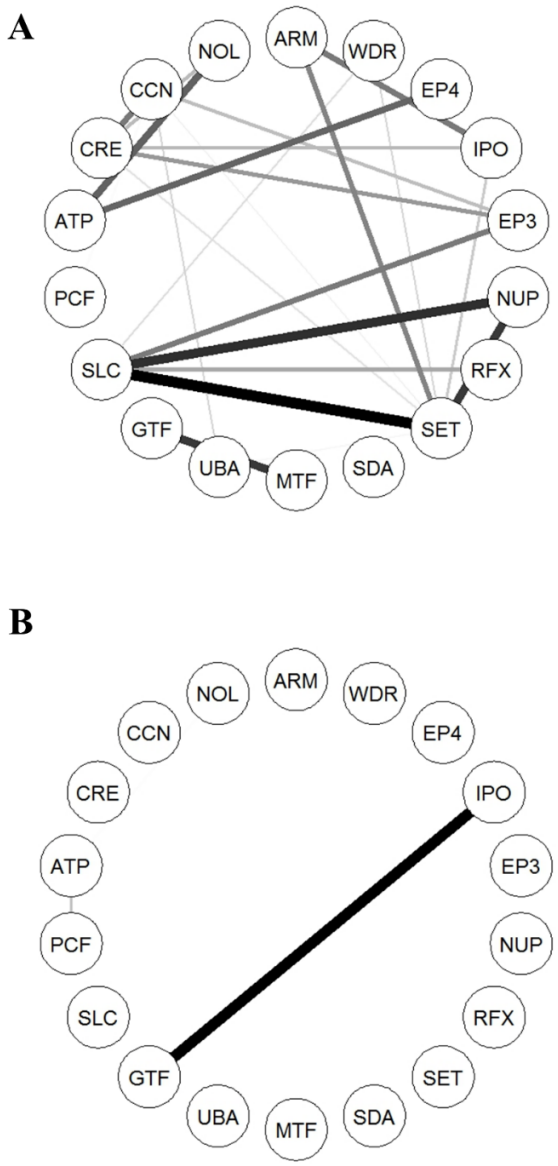

A. Sham-treated IBCs from childhood asthmatics

B. Dex-treated IBCs from childhood asthmatics

For clarity, only the edges corresponding to the Pearson correlation coefficient > 0.8 were shown. The edge width is proportional to the Pearson correlation coefficient between two nodes. The network was visualized using qgraph R package.

ARM, *ARMC5;* ATP, *ATP2A2;* CCN, *CCNK;* CRE, *CREBBP;* EP3, *EP300;* EP4, *EP400;* GTF, *GTF3C1;* IPO, *IPO13;* MTF, *MTF1;* NOL, *NOL8;* NUP, *NUP188;* PCF, *PCF11;* RFX, *RFX5;* SDA, *SDAD1;* SET, *SETD1A;* SLC, *SLC25A22;* UBA, *UBAP2L;* WDR, *WDR59*

Figure 10. Scatter plot of module eigengenes in the blue module (childhood asthmatics-specific gene module)

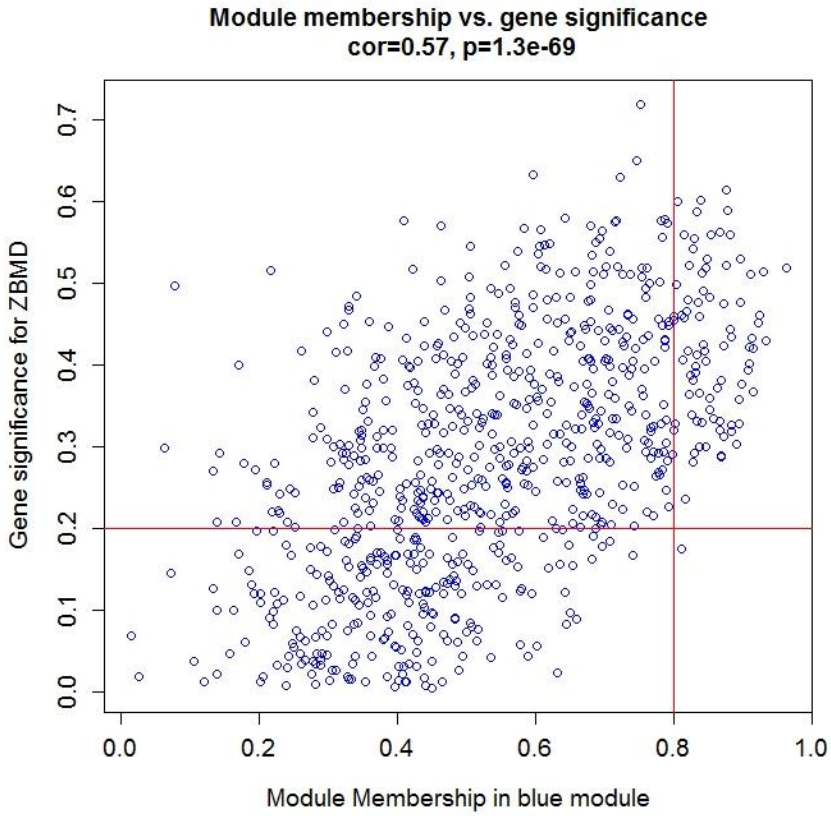

Hub genes are located at the right and upper quadrant.

References

1. Weinstein RS. Clinical practice. Glucocorticoid-induced bone disease. N Engl J Med. 2011;365(1):62-70.

2. Kelly HW, Van Natta ML, Covar RA, Tonascia J, Green RP, Strunk RC, et al. Effect of long-term corticosteroid use on bone mineral density in children: a prospective longitudinal assessment in the childhood Asthma Management Program (CAMP) study. Pediatrics. 2008;122(1):e53-61.

3. Canalis E, Delany AM. Mechanisms of glucocorticoid action in bone. Ann N Y Acad Sci. 2002;966:73-81.

4. Huang QY, Recker RR, Deng HW. Searching for osteoporosis genes in the post-genome era: progress and challenges. Osteoporos Int. 2003;14(9):701-15.

5. Manenschijn L, van den Akker EL, Lamberts SW, van Rossum EF. Clinical features associated with glucocorticoid receptor polymorphisms. An overview. Ann N Y Acad Sci. 2009;1179:179-98.

6. Quax RA, Manenschijn L, Koper JW, Hazes JM, Lamberts SW, van Rossum EF, et al. Glucocorticoid sensitivity in health and disease. Nat Rev Endocrinol. 2013;9(11):670-86.

7. Park HW, Ge B, Tse S, Grundberg E, Pastinen T, Kelly HW, et al. Genetic risk factors for decreased bone mineral accretion in children with asthma receiving multiple oral corticosteroid bursts. J Allergy Clin Immunol.

2015;136(5):1240-6 e1-8.

8. Jones TS, Kaste SC, Liu W, Cheng C, Yang W, Tantisira KG, et al. CRHR1 polymorphisms predict bone density in survivors of acute lymphoblastic leukemia. J Clin Oncol. 2008;26(18):3031-7.

9. Park HW, Tse S, Yang W, Kelly HW, Kaste SC, Pui CH, et al. A genetic factor associated with low final bone mineral density in children after a long-term glucocorticoids treatment. Pharmacogenomics J. 2017;17(2):180-5.

10. Carter SL, Brechbuhler CM, Griffin M, Bond AT. Gene co-expression network topology provides a framework for molecular characterization of cellular state. Bioinformatics. 2004;20(14):2242-50.

11. Stuart JM, Segal E, Koller D, Kim SK. A gene-coexpression network for global discovery of conserved genetic modules. Science. 2003;302(5643):249-55.

12. Jeong H, Mason SP, Barabasi AL, Oltvai ZN. Lethality and centrality in protein networks. Nature. 2001;411(6833):41-2.

13. Hartwell LH, Hopfield JJ, Leibler S, Murray AW. From molecular to modular cell biology. Nature. 1999;402(6761 Suppl):C47-52.

14. Zhang B, Horvath S. A general framework for weighted gene co-expression network analysis. Stat Appl Genet Mol Biol. 2005;4:Article17.

15. Clarke C, Madden SF, Doolan P, Aherne ST, Joyce H, O'Driscoll L, et al. Correlating transcriptional networks to breast cancer survival: a large-scale coexpression analysis. Carcinogenesis. 2013;34(10):2300-8.

16. Ren Y, Cui Y, Li X, Wang B, Na L, Shi J, et al. A co-expression network analysis reveals lncRNA abnormalities in peripheral blood in early-onset schizophrenia. Prog Neuropsychopharmacol Biol Psychiatry. 2015;63:1-5.

17. Zheng X, Xue C, Luo G, Hu Y, Luo W, Sun X. Identification of crucial genes in intracranial aneurysm based on weighted gene coexpression network analysis. Cancer Gene Ther. 2015;22(5):238-45.

18. Guo Y, Ma J, Xiao L, Fang J, Li G, Zhang L, et al. Identification of key pathways and genes in different types of chronic kidney disease based on WGCNA. Mol Med Rep. 2019;20(3):2245-57.

19. Liu Z, Li M, Fang X, Shen L, Yao W, Fang Z, et al. Identification of surrogate prognostic biomarkers for allergic asthma in nasal epithelial brushing samples by WGCNA. J Cell Biochem. 2019;120(4):5137-50.

20. Zeng Y, Zhang L, Zhu W, Xu C, He H, Zhou Y, et al. Quantitative proteomics and integrative network analysis identified novel genes and pathways related to osteoporosis. J Proteomics. 2016;142:45-52.

21. Qin L, Liu Y, Wang Y, Wu G, Chen J, Ye W, et al. Computational Characterization of Osteoporosis Associated SNPs and Genes Identified by Genome-Wide Association Studies. PLoS One. 2016;11(3):e0150070.

22. Li JJ, Wang BQ, Fei Q, Yang Y, Li D. Identification of candidate genes in osteoporosis by integrated microarray analysis. Bone Joint Res. 2016;5(12):594-601.

23. Farber CR. Identification of a gene module associated with BMD through the integration of network analysis and genome-wide association data. J Bone Miner Res. 2010;25(11):2359-67.

24. Chen YC, Guo YF, He H, Lin X, Wang XF, Zhou R, et al. Integrative Analysis of Genomics and Transcriptome Data to Identify Potential Functional Genes of BMDs in Females. J Bone Miner Res. 2016;31(5):1041-9.

25. Childhood Asthma Management Program Research G, Szefler S, Weiss S, Tonascia J, Adkinson NF, Bender B, et al. Long-term effects of budesonide or nedocromil in children with asthma. N Engl J Med. 2000;343(15):1054-63.

26. Sambrook PN. How to prevent steroid induced osteoporosis. Ann Rheum Dis. 2005;64(2):176-8.

27. Subramanian A, Tamayo P, Mootha VK, Mukherjee S, Ebert BL, Gillette MA, et al. Gene set enrichment analysis: a knowledge-based approach for interpreting genome-wide expression profiles. Proc Natl Acad Sci U S A. 2005;102(43):15545-50.

28. Harris PS, Venkataraman S, Alimova I, Birks DK, Balakrishnan I, Cristiano B, et al. Integrated genomic analysis identifies the mitotic checkpoint kinase WEE1 as a novel therapeutic target in medulloblastoma. Mol Cancer. 2014;13:72.

29. Qiu W, Rogers AJ, Damask A, Raby BA, Klanderman BJ, Duan QL, et al. Pharmacogenomics: novel loci identification via integrating gene

differential analysis and eQTL analysis. Hum Mol Genet. 2014;23(18):5017-24.

30. Langfelder P, Horvath S. WGCNA: an R package for weighted correlation network analysis. BMC Bioinformatics. 2008;9:559.

31. Langfelder P, Horvath S. Eigengene networks for studying the relationships between co-expression modules. BMC Syst Biol. 2007;1:54.

32. Ritchie SC, Watts S, Fearnley LG, Holt KE, Abraham G, Inouye M. A Scalable Permutation Approach Reveals Replication and Preservation Patterns of Network Modules in Large Datasets. Cell Syst. 2016;3(1):71-82.

33. Gene Expression Omnibus, GSE21727. Available at: https://www.ncbi.nlm.nih.gov/geo/query/acc.cgi?acc=GSE21727. Accessed November 14, 2019. .

34. Reimand J, Arak T, Adler P, Kolberg L, Reisberg S, Peterson H, et al. g:Profiler-a web server for functional interpretation of gene lists (2016 update). Nucleic Acids Res. 2016;44(W1):W83-9.

35. Zhang K, Chang S, Cui S, Guo L, Zhang L, Wang J. ICSNPathway: identify candidate causal SNPs and pathways from genome-wide association study by one analytical framework. Nucleic Acids Res. 2011;39(Web Server issue):W437-43.

36. Xiao H, Shan L, Zhu H, Xue F. Detection of significant pathways in osteoporosis based on graph clustering. Mol Med Rep. 2012;6(6):1325-32.

37. Gene Ontology Browser, GO:0044237. Available at:

http://www.informatics.jax.org/vocab/gene_ontology/GO:0044237. . Accessed November 14, 2019.

38. Florencio-Silva R, Sasso GR, Sasso-Cerri E, Simoes MJ, Cerri PS. Biology of Bone Tissue: Structure, Function, and Factors That Influence Bone Cells. Biomed Res Int. 2015;2015:421746.

39. Marks SC, Jr., Popoff SN. Bone cell biology: the regulation of development, structure, and function in the skeleton. Am J Anat. 1988;183(1):1-44.

40. Goodman RH, Smolik S. CBP/p300 in cell growth, transformation, and development. Genes Dev. 2000;14(13):1553-77.

41. Hu Z, Wang Y, Sun Z, Wang H, Zhou H, Zhang L, et al. miRNA-132-3p inhibits osteoblast differentiation by targeting Ep300 in simulated microgravity. Sci Rep. 2015;5:18655.

42. Berendsen AD, Olsen BR. Osteoblast-adipocyte lineage plasticity in tissue development, maintenance and pathology. Cell Mol Life Sci. 2014;71(3):493-7.

43. Nishikawa K, Nakashima T, Takeda S, Isogai M, Hamada M, Kimura A, et al. Maf promotes osteoblast differentiation in mice by mediating the age-related switch in mesenchymal cell differentiation. J Clin Invest. 2010;120(10):3455-65.

44. Wu M, Chen G, Li YP. TGF-beta and BMP signaling in osteoblast, skeletal development, and bone formation, homeostasis and disease. Bone Res.

2016;4:16009.

45. Yang D, Guo J, Divieti P, Shioda T, Bringhurst FR. CBP/p300-interacting protein CITED1 modulates parathyroid hormone regulation of osteoblastic differentiation. Endocrinology. 2008;149(4):1728-35.

46. Knutti D, Kaul A, Kralli A. A tissue-specific coactivator of steroid receptors, identified in a functional genetic screen. Mol Cell Biol. 2000;20(7):2411-22.

47. Kino T, Nordeen SK, Chrousos GP. Conditional modulation of glucocorticoid receptor activities by CREB-binding protein (CBP) and p300. J Steroid Biochem Mol Biol. 1999;70(1-3):15-25.

48. Mullighan CG, Zhang J, Kasper LH, Lerach S, Payne-Turner D, Phillips LA, et al. CREBBP mutations in relapsed acute lymphoblastic leukaemia. Nature. 2011;471(7337):235-9.

49. Lu NZ, Cidlowski JA. Glucocorticoid receptor isoforms generate transcription specificity. Trends Cell Biol. 2006;16(6):301-7.

50. Assie G, Libe R, Espiard S, Rizk-Rabin M, Guimier A, Luscap W, et al. ARMC5 mutations in macronodular adrenal hyperplasia with Cushing's syndrome. N Engl J Med. 2013;369(22):2105-14.

51. Kaltsas G, Makras P. Skeletal diseases in Cushing's syndrome: osteoporosis versus arthropathy. Neuroendocrinology. 2010;92 Suppl 1:60-4.

52. Tao T, Lan J, Lukacs GL, Hache RJ, Kaplan F. Importin 13 regulates nuclear import of the glucocorticoid receptor in airway epithelial cells. Am J

Respir Cell Mol Biol. 2006;35(6):668-80.

53. Al-Barghouthi BM, Farber CR. Dissecting the Genetics of Osteoporosis using Systems Approaches. Trends Genet. 2019;35(1):55-67.

54. Zhang B, Gaiteri C, Bodea LG, Wang Z, McElwee J, Podtelezhnikov AA, et al. Integrated systems approach identifies genetic nodes and networks in late-onset Alzheimer's disease. Cell. 2013;153(3):707-20.

55. Makinen VP, Civelek M, Meng Q, Zhang B, Zhu J, Levian C, et al. Integrative genomics reveals novel molecular pathways and gene networks for coronary artery disease. PLoS Genet. 2014;10(7):e1004502.

56. Mohr S, Liew CC. The peripheral-blood transcriptome: new insights into disease and risk assessment. Trends Mol Med. 2007;13(10):422-32.

57. Gordon S, Taylor PR. Monocyte and macrophage heterogeneity. Nat Rev Immunol. 2005;5(12):953-64.

58. Bonjour JP, Chevalley T, Ferrari S, Rizzoli R. The importance and relevance of peak bone mass in the prevalence of osteoporosis. Salud Publica Mex. 2009;51 Suppl 1:S5-17.

59. Deng FY, Lei SF, Zhang Y, Zhang YL, Zheng YP, Zhang LS, et al. Peripheral blood monocyte-expressed ANXA2 gene is involved in pathogenesis of osteoporosis in humans. Mol Cell Proteomics. 2011;10(11):M111 011700.

60. Ralston SH, Galwey N, MacKay I, Albagha OM, Cardon L, Compston JE, et al. Loci for regulation of bone mineral density in men and women

identified by genome wide linkage scan: the FAMOS study. Hum Mol Genet. 2005;14(7):943-51.

61. Reynolds LM, Taylor JR, Ding J, Lohman K, Johnson C, Siscovick D, et al. Age-related variations in the methylome associated with gene expression in human monocytes and T cells. Nat Commun. 2014;5:5366.

62. Stuss M, Rieske P, Ceglowska A, Stepien-Klos W, Liberski PP, Brzezianska E, et al. Assessment of OPG/RANK/RANKL gene expression levels in peripheral blood mononuclear cells (PBMC) after treatment with strontium ranelate and ibandronate in patients with postmenopausal osteoporosis. J Clin Endocrinol Metab. 2013;98(5):E1007-11.

63. Chapin WJ, Lenkala D, Mai Y, Mao Y, White SR, Huang RS. Peripheral blood IRF1 expression as a marker for glucocorticoid sensitivity. Pharmacogenet Genomics. 2015;25(3):126-33.

64. Chelly J, Kaplan JC, Maire P, Gautron S, Kahn A. Transcription of the dystrophin gene in human muscle and non-muscle tissue. Nature. 1988;333(6176):858-60.

65. Kimoto Y. A single human cell expresses all messenger ribonucleic acids: the arrow of time in a cell. Mol Gen Genet. 1998;258(3):233-9.

66. Liew CC, Ma J, Tang HC, Zheng R, Dempsey AA. The peripheral blood transcriptome dynamically reflects system wide biology: a potential diagnostic tool. J Lab Clin Med. 2006;147(3):126-32.

67. Komano Y, Nanki T, Hayashida K, Taniguchi K, Miyasaka N.

Identification of a human peripheral blood monocyte subset that differentiates into osteoclasts. Arthritis Res Ther. 2006;8(5):R152.

68. Sabokbar A, Athanasou NS. Generating human osteoclasts from peripheral blood. Methods Mol Med. 2003;80:101-11.

69. Becerikli M, Jaurich H, Schira J, Schulte M, Dobele C, Wallner C, et al. Age-dependent alterations in osteoblast and osteoclast activity in human cancellous bone. J Cell Mol Med. 2017;21(11):2773-81.

70. Lai P, Song Q, Yang C, Li Z, Liu S, Liu B, et al. Loss of Rictor with aging in osteoblasts promotes age-related bone loss. Cell Death Dis. 2016;7(10):e2408.

71. Buchman AL. Side effects of corticosteroid therapy. J Clin Gastroenterol. 2001;33(4):289-94.

국문초록

천식 환자에서 스테로이드 사용에 따른 골밀도 변화 관련 주요 생물학적 경로 발굴

이 서 영

서울대학교 대학원

의학과 협동과정 임상약리학 전공

서론: 골밀도 감소는 장기간 전신 스테로이드 사용의 잘 알려진 부작용이나 개인마다 그 감수성의 차이가 있다. 이러한 개인적 감수성을 유전적 소인으로 설명하기 위한 연구가 그 동안 많이 진행되어 왔다. 그러나 스테로이드를 치료의 근간으로 하는 천식 환자에서 골밀도 변화의 생물학적 기전을 포괄적으로 밝힌 연구는 아직 없다. 본 연구에서는 전신 스테로이드를 투여 받은 천식 환자의 말초 혈액의 전장 유전자 발현을 네트워크에 기초한 방법으로 분석하여 골밀도 감소와 관련된 생물학적 경로를 발굴하고자 하였다.

방법: 소아 천식 코호트에 등록되어 급성 악화 시 2 mg/kg의 고용량 경구 스테로이드를 2일 이상 투여 받은 32명의 소아 천식 환자의 불멸화 B세포(IBC, immortalized B cells)와, 1년 이상 매일 경구 프레드니솔론 15mg 이상을 투여 받은 17명의 성인 천식 환자의 말초혈액단핵세포(PBMC, peripheral blood mononuclear cells)에서 전장 유전자 발현을 조사하였다. 가중 유전자 동시발현 네트워크 분석(WGCNA, weighted gene co-expression analysis)를 이용하여 서로 긴밀하게 연결된 유전자 모듈(gene module)을 확인하였고, 모듈의 고유유전자값(eigengene value)과 스테로이드에 의한 골밀도 감소와의 상관관계를 확인하여 골밀도 감소와 연관된 모듈을 발굴하였다. 이어 발굴된 모듈이 다른 인구집단인 성인 천식 환자에서도 의미가 있는지 확인하였다. 즉 모듈의 구조가 성인 천식 유전자 발현 프로필에서도 보존이 되는 지와 스테로이드 투여에 의한 골밀도 감소와 유의한 상관성을 가지는지 찾아 보았다. 마지막으로 발굴된 모듈에 속하는 유전자를 대상으로 관련된 생물학적 경로를 확인하였다.

결과: 소아 천식 IBC와 성인 천식 환자 PBMC 전장 유전자 발현 사이에 상관도가 좋은 5,000개의 유전자를 선정하여 WGCNA 분석을

시행하였다. 소아 천식 환자 유전자 발현 WGCNA 분석을 통하여 10개의 유전자 모듈을 찾았으며 이 중 2개의 모듈의 고유유전자 값이 급성 악화로 인하여 스테로이드 치료를 받은 후의 골밀도 Z값과의 유의한 상관관계를 보이는 것을 확인하였다. 소아 천식에서 발견된 2개의 유전자 모듈 중 199개 유전자로 구성된 모듈의 구조가 성인 천식 환자 PBMC 유전자 발현에서도 잘 유지되고 동시에 장기간의 경구 스테로이드 치료를 받은 뒤의 골밀도 Z값과도 유의한 상관관계를 가진다는 것을 알 수 있었다. 이렇게 발굴된 모듈을 구성하는 199개의 유전자를 대상으로 유전자 세트 농축 분석(gene set enrichment analysis)을 시행한 결과 해당 모듈이 유전자 온톨로지 모델에서 세포대사경로에 농축됨을 확인하였다. 또한 이 모듈의 특성을 잘 반영하는 18개의 허브 유전자(*ARMC5, ATP2A2, CCNK, CREBBP, EP300, EP400, GTF3C1, IPO13, MTF1, NOL8, NUP188, PCF11, RFX5, SDAD1, SETD1A, SLC25A22, UBAP2L, WDR59*)를 찾을 수 있었다.

결론: 소아와 성인 천식 환자 말초 혈액 유전자 발현의 네트워크 분석을 통해 스테로이드 투여에 따른 골밀도 저하와 유의한 상관을 보이는 유전자 모듈을 발굴하였으며 이 모듈의 유전자는 유전자

온톨로지 상 세포대사경로에 중요하게 관여함을 확인하였다. 이 연구를 통해 밝혀진 생물학적 경로는 스테로이드에 의한 골밀도 감소의 병인에서 중요한 역할을 할 것으로 생각된다.

주요어 : 천식, 유전자 경로, Gene set enrichment analysis, 시스템 생물학, 유전자 전사체 분석, Weighted gene co-expression network analysis